Protein Phosphatase 2A Catalytic Subunit α Plays a MyD88-Dependent, Central Role in the Gene-Specific Regulation of Endotoxin Tolerance

Ling Xie,[1,5] Cui Liu,[1,5] Li Wang,[1,4] Harsha P. Gunawardena,[1] Yanbao Yu,[1] Ruyun Du,[4] Debra J. Taxman,[3] Penggao Dai,[1] Zhen Yan,[1] Jing Yu,[1] Stephen P. Holly,[1] Leslie V. Parise,[1] Yisong Y. Wan,[2,3] Jenny P. Ting,[2,3] and Xian Chen[1,2,4,*]
[1]Department of Biochemistry and Biophysics
[2]Lineberger Comprehensive Cancer Center
[3]Department of Microbiology and Immunology
University of North Carolina, Chapel Hill, NC 27599, USA
[4]Department of Chemistry, Fudan University, Shanghai 20032, China
[5]These authors contributed equally to this work
*Correspondence: xianc@email.unc.edu
http://dx.doi.org/10.1016/j.celrep.2013.01.029

SUMMARY

MyD88, the intracellular adaptor of most TLRs, mediates either proinflammatory or immunosuppressive signaling that contributes to chronic inflammation-associated diseases. Although gene-specific chromatin modifications regulate inflammation, the role of MyD88 signaling in establishing such epigenetic landscapes under different inflammatory states remains elusive. Using quantitative proteomics to enumerate the inflammation-phenotypic constituents of the MyD88 interactome, we found that in endotoxin-tolerant macrophages, protein phosphatase 2A catalytic subunit α (PP2Ac) enhances its association with MyD88 and is constitutively activated. Knockdown of PP2Ac prevents suppression of proinflammatory genes and resistance to apoptosis. Through site-specific dephosphorylation, constitutively active PP2Ac disrupts the signal-promoting TLR4-MyD88 complex and broadly suppresses the activities of multiple proinflammatory/proapoptotic pathways as well, shifting proinflammatory MyD88 signaling to a prosurvival mode. Constitutively active PP2Ac translocated with MyD88 into the nuclei of tolerant macrophages establishes the immunosuppressive pattern of chromatin modifications and represses chromatin remodeling to selectively silence proinflammatory genes, coordinating the MyD88-dependent inflammation control at both signaling and epigenetic levels under endotoxin-tolerant conditions.

INTRODUCTION

Toll-like receptors (TLRs) activate the innate immune system by mounting appropriate inflammatory responses to contain infection or repair damaged tissues (Drexler and Foxwell, 2010). To avoid harmful effects of persistent signaling caused by the continual presence of stimuli, cells become transiently unresponsive by acquiring tolerance to chronic inflammation, leading to a negative consequence that tumor cells can escape immunosurveillance (Rakoff-Nahoum and Medzhitov, 2009). In transmitting inflammatory signals, by mechanisms yet to be elucidated, the intracellular adaptor protein MyD88 (myeloid differentiation primary response 88) of most TLRs acts as a double-edged sword promoting both protective and harmful inflammation (Huang et al., 2008).

Recent work has revealed that inflammation control is achieved by a gene-specific mechanism in which distinct chromatin modifications contribute to selective silencing of TLR4-induced proinflammatory or tolerizable (T class) genes under an endotoxin tolerance (ET)-associated chronic inflammatory state (Foster et al., 2007). Major questions remain unanswered including the following:

(1) How does MyD88 mediate both acute and chronic inflammatory responses?
(2) What is the driving force for "converting" proinflammatory MyD88 to an immunosuppressive mediator?
(3) How are distinct, inflammation-specific patterns of chromatin modifications differentially established at the T class promoters?

Emerging evidence suggests that an effective, unharmful inflammatory response is intrinsically regulated by subtly distinct intracellular protein interactions, i.e., "interactomes" (protein-protein interaction network) involved in signal transduction (Liew et al., 2005). During TLR signaling, MyD88 serves as a scaffold that coordinates protein complex assembly through sequential recruitment of specific proteins varying from TLR molecules to downstream proteins (Dai et al., 2009; Wang et al., 2006). Based on our previous identification of multiple signal regulators that interact with MyD88 in a timely and orderly manner to tightly regulate the amplitude and duration of TLR signaling (Dai et al., 2009), we reason that MyD88 may regulate either acute or chronic inflammation via assembling different, inflammation-phenotypic interactomes.

RESULTS

As a Core Component of MyD88 Interactome in ET Macrophages, PP2Ac Is Chronically Activated

First, by using our amino-acid-coded mass tagging (AACT)-based quantitative proteomic approach (Chen et al., 2000) with modifications for interactome screening (Figure 1A), we dissected the MyD88-interacting complexes assembled in RAW cells under different inflammatory states including (1) no stimulation (N), (2) challenging with a single high LPS dose (LPS responsive, NL), (3) priming with a low LPS dose (LPS tolerant, T), and (4) challenging T cells with a high-dose LPS (TL). Compared to NL cells, T or TL cells showed an ET-specific phenotype of immunosuppression and resistance to apoptosis (Figure S1A). Through phenotypic interactome analysis (Figure 1A), we found that MyD88 interacts with different sets of proteins in NL versus TL macrophages (unpublished data): together with many negative immune regulators (Liew et al., 2005) including a negative TLR regulator *Flii* (Wang et al., 2006), protein phosphatase catalytic subunit α (PP2Ac) was found recruited into the MyD88 interactome specifically in ET cells (Figures 1B and S1B). Because approximately 20% of the components in the TL-specific MyD88 interactome contain the domains interacting with PP2Ac (Figure S1C) that is generally considered as a suppressor of proinflammatory kinases (Junttila et al., 2008), this inflammation-phenotypic proteomic finding suggested that PP2Ac plays a central, MyD88-dependent, immunosuppressive role during ET.

Given that neither expression nor stability of PP2Ac was affected by LPS-induced inflammation (Figure S2A), we compared the PP2Ac activity in RAW cells under different inflammatory conditions. Compared to naive (N) cells, whereas its activity was little changed under NL, PP2Ac was highly activated with a prolonged stimulation and was sustained under TL (Figure 1C), indicating the activity-based, inflammation-phenotypic function of PP2Ac. To clarify the MyD88 dependence of PP2Ac activation, we measured PP2Ac activity in paired wild-type (WT) and MyD88-depleted ($MyD88^{-/-}$) (Figure S2B) bone marrow-derived macrophages (BMDMs) under different inflammatory states induced by a variety of TLR agonists. Similar to RAWs, PP2Ac activity showed a 2-fold increase in TL WT BMDMs but less than 10% changes in $MyD88^{-/-}$ BMDMs under N, NL, and TL (Figure 1D). The TLR9 agonist CpG, which triggers only MyD88-dependent pathways, induced a greater increase in PP2Ac activity in TL WT BMDMs than that induced by LPS, which activates both MyD88-dependent and -independent pathways (Figure 1E), whereas no differences in PP2Ac activity were observed between WT and $MyD88^{-/-}$ BMDMs when the TLR3 agonist Poly (I:C) stimulated only MyD88-independent pathways (Figure 1F). These agonist-specific effects indicated the MyD88-dependent activation of PP2Ac in chronically inflamed cells. Second, to clarify how PP2Ac activity is regulated in tolerant macrophages, we respectively used either LPS-conditioned medium, i.e., that separated from the LPS-pretreated RAWs, or TNF-α or ionizing radiation (IR) to trigger inflammation in BMDMs. Under chronic exposure, all non-TLR stimuli caused a similar degree of tolerance-specific activation of PP2Ac in both WT and $MyD88^{-/-}$ BMDMs (Figure 1G). In a coordinate manner,

unlike its LPS-inducible nature in WT but not in $MyD88^{-/-}$ BMDMs (Figure 1H, left), phospho-p65 triggered by non-TLR stimuli showed similar time-dependent induction in both types of BMDMs (Figure 1H, right), indicating that stimuli-induced, secondary, NFκB-regulated production of inflammatory cytokines such as TNF-α causes tolerance-specific PP2Ac activation. Because TNF-α is a T class gene and its release is MyD88 promoted (Figure S2B), this secondary effect on PP2Ac activation was therefore more pronounced in the WT BMDMs directly stimulated by the TLR agonists that trigger MyD88-dependent pathways for producing these T class cytokines. Only during the chronic inflammation mediated by TLR2/TLR4/TR9 is the sustained PP2Ac activation MyD88 dependent.

Constitutively Active PP2Ac Regulates Immunosuppression during ET

To determine the correlation of persistently or constitutively activated PP2Ac with immunosuppression, we measured cytokine release from stable RAW lines expressing either shRNA for knocking down PP2Ac (PP2Ac knockdown [KD]) or shRNA for GFP (WT control) (Figures 2A and S2C). Under NL, most cytokines showed LPS-inducible release in both PP2Ac KD and WT RAWs (Figure 2B). In contrast, compared to the LPS-tolerized WT RAWs showing reduced production of T class cytokines, the LPS-primed PP2Ac KD cells were hyperresponsive to high-dose LPS stimulation and released greater amounts of cytokines. Furthermore, we determined the effect of constitutively active PP2Ac on the expression of 84 mouse genes encoding inflammatory factors, most known to be regulated by NFκB (Figure S2D). Compared with their levels in WT RAWs, 34 out of 84 genes showed more than a 30% increase (Table S1), some of which were validated by qPCR (Figure 2B). Also, T class genes (*IL6* or *IL10*) had dramatically enhanced expression in the PP2Ac KD cells even under TL, reversing their suppressed expression in TL WT cells. In contrast, under NL or TL, PP2Ac KD had little effect on the LPS-inducible trend of *Fpr1* (Figure 2B), a nontolerizeable gene (Foster et al., 2007), suggesting that constitutively active PP2Ac is involved specifically in T class gene regulation under ET.

Furthermore, to determine whether the constitutively active form of PP2Ac directly contributes to acquiring ET, we transfected constructs expressing either WT or a dominant-negative (DN) mutant of PP2Ac (Chang et al., 2011) into the PP2Ac KD RAWs. Under TL, whereas expression of WT PP2Ac restored the tolerance with reduced *IL6*, the PP2Ac DN mutant with similar expression failed to suppress this T class gene (Figure 2C), indicating that constitutively active PP2Ac participates in the gene-specific control of chronic inflammation by selectively suppressing T class genes.

Constitutively Active PP2Ac Promotes the MyD88-Dependent Survival of ET Cells through Broadly Targeting Proinflammatory Kinases and Proapoptotic Factors

To identify PP2Ac-target pathways through which ET is regulated by constitutively active PP2Ac, we profiled the phosphoproteomic changes in PP2Ac KD versus WT RAWs under TL (Figure S3A). Some of the PP2Ac-target sites
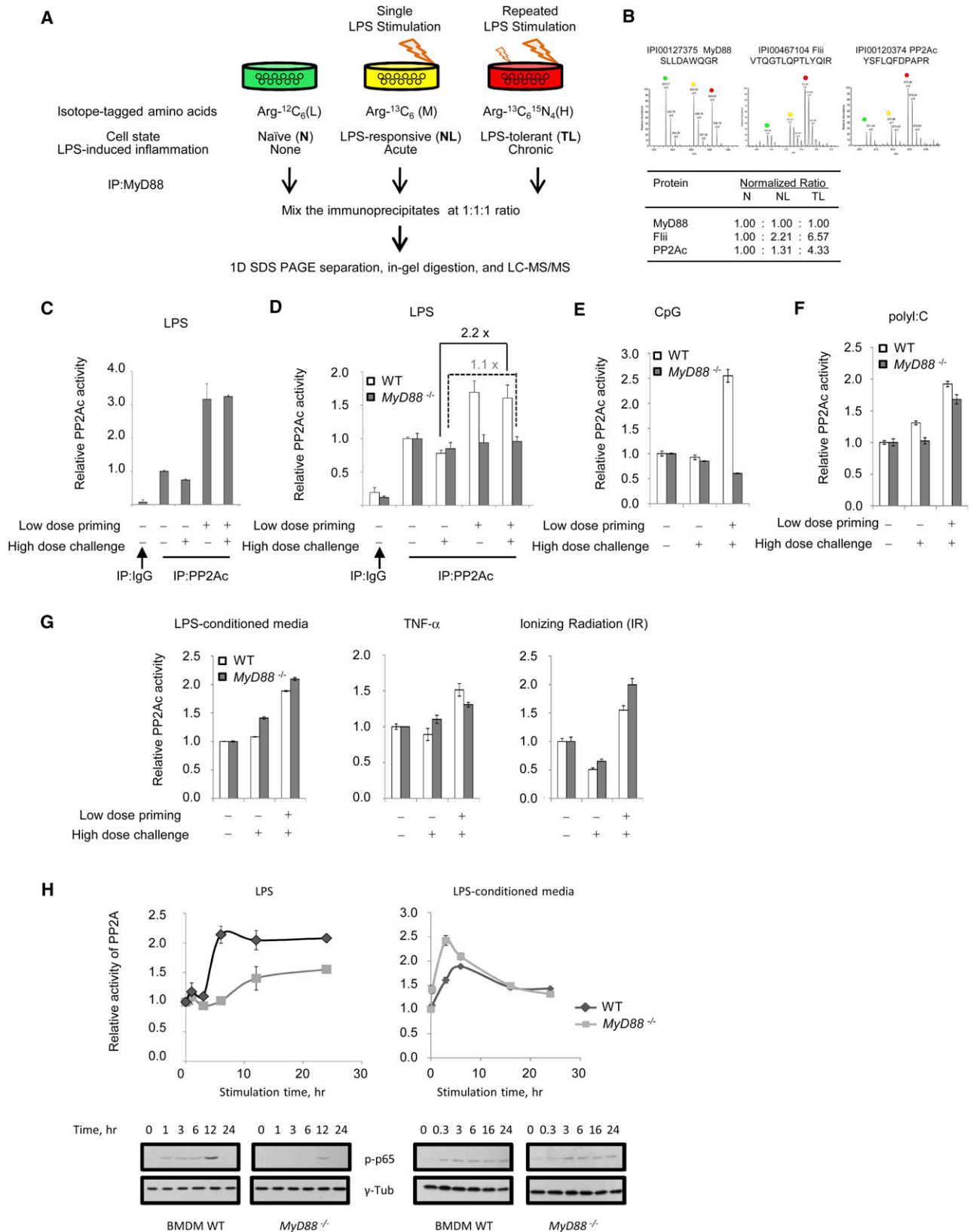
(legend on next page)

(Figure S3B) that were identified based on their phosphorylation increases in TL PP2Ac-depleted cells were in the components of the TL-specific MyD88 interactome (Figure S1B), including Rps6 (a substrate of p70S6K), Rap1 (a MAPK component), Akt1, and a mTORC1/C2 component Raptor, revealing that through site-specific dephosphorylation, constitutively active PP2Ac represses the proinflammatory/proapoptotic activity of the PI3K-mTOR-p70S6K-Akt pathway. In addition, we found that constitutively active PP2Ac targeted AP1/c-Jun, the mediator of stimuli-induced apoptosis (Li et al., 2004) (Figure S3C): under TL, in contrast to its decreased abundance in WT RAWs, phosphorylation of c-Jun Ser63 was significantly increased when PP2Ac was depleted (Figure 2D). Thus, similar to the antiapoptotic nature of PP2A (Kong et al., 2004), PP2Ac, when constitutively activated, negatively regulates the proapoptotic activity of c-Jun by directly dephosphorylating its proapoptotic pSer63.

We next determined how PP2Ac KD affects the ET-characteristic resistance to apoptosis. First, we evaluated cell survival/proliferation in PP2Ac KD RAWs under N, NL, and TL in the presence of cycloheximide (CHX) that can amplify LPS-induced apoptosis (Suzuki et al., 2004). Compared with the ET-specific increase of the surviving WT cells, PP2Ac KD led to reduced colony formation, indicating an increase in apoptotic/dead cells even under TL (Figure 2E). Similarly, in flow cytometry analysis, consistent with what was shown for cytokine release (Figure 2B), PP2Ac KD RAWs showed some degree of LPS-inducible apoptosis/cell death even in nonstimulated cells (Figure 2F), indicating the cell sensitization due to PP2Ac depletion. The NL WT RAWs showed LPS-inducible apoptosis, whereas this induction was suppressed under TL. In contrast, a dramatically increased susceptibility to apoptosis was observed even for T or TL PP2Ac KD cells. The consistent results from both assays (Figures 2E and 2F) indicated that PP2Ac depletion reduces the resistance of ET macrophages to apoptosis.

Furthermore, because MyD88 promotes tumor growth by either modulating particular kinase pathways (Lee et al., 2010) or inhibiting apoptosis (Rakoff-Nahoum and Medzhitov, 2007), we next examined whether the PP2Ac effect on apoptotic propensity is MyD88 dependent. Because PP2Ac is highly abundant and robust, and nondividing BMDMs have extremely low transfection efficiency and shRNA stability, very low percentages of endogenous PP2Ac KD could be achieved in BMDMs (data not shown). Given that the phosphatase inhibitor okadaic acid (OA) at concentrations <50 nM showed greater specificity in inhibiting the activity of PP2Ac to that of PP2Ac DN (Chang et al., 2011), we used 20 nM OA to mimic PP2Ac KD in the experiments involving BMDMs. Accordingly, we observed similar increases of c-Jun pSer63 in either PP2Ac KD RAW or OA-treated BMDMs, both under TL (Figures 2D and S3C). Addition-

ally, under T or TL, both WT and PP2Ac KD RAWs pretreated with 20 nM OA showed similar changes in the populations of apoptotic/dead cells (Figure 2F, middle versus bottom row). All these similarities in OA treatment and shRNA-mediated PP2Ac KD on promoting apoptosis indicated the specificity of 20 nM OA in inhibiting constitutively active PP2Ac.

We therefore used 20 nM OA to investigate the MyD88 dependence of the PP2Ac effect in primary WT versus $MyD88^{-/-}$ BMDMs. Accordingly, similar to WT RAWs, more WT BMDMs underwent apoptosis/death under NL than those under TL (Figure S3D). Conversely, viability of $MyD88^{-/-}$ BMDMs was unaffected by either NL or TL. Furthermore, OA-mediated PP2Ac inhibition triggered more apoptosis/death of TL WT but not $MyD88^{-/-}$ BMDMs. Furthermore, compared to their untreated counterparts, the OA-treated WT BMDMs under TL showed features typical of mitochondrial-mediated apoptosis, including greater cleavage of caspase-3 and PARP, and higher expression of the proapoptotic proteins Bak and Bax (Figure 2G). In contrast, such an OA-initiated apoptosis in TL cells was abolished in $MyD88^{-/-}$ BMDMs. Because c-Jun pSer63 is upstream of caspase-3 activation during apoptosis (Li et al., 2004), analysis of multiple, interconnected pathway-specific apoptotic markers thus indicated that constitutively active PP2Ac promotes cell survival in a MyD88-dependent manner.

Constitutively Active PP2Ac Dissociates the Signal-Promoting TLR4-MyD88 Complex through Dephosphorylating Key Serines in the Toll/IL-1 Receptor Domain of MyD88

We next investigated the role of TL-specific PP2Ac-MyD88 interaction (Figure 3A, left) in acquiring ET. First, we found that MyD88 binds to the WT PP2Ac more tightly than to the PP2Ac DN under TL (Figure 3A, right), indicating that MyD88 interacts only with constitutively active PP2Ac. Furthermore, to identify exactly where constitutively active PP2Ac targets MyD88, we employed an AACT-based quantitative proteomics approach where tagged MyD88 expressed in HEK TLR4 stable cells was immunoprecipitated (IP) for MS analysis because no phosphorylation on endogenous MyD88 was detected in the phosphoproteomic analysis above. Meanwhile, we used 20 nM OA to highlight PP2Ac-target phospho-sites on MyD88. In MyD88 immunoprecipitates from differentially stimulated TLR4 stable cells, with or without 20 nM OA treatment, we identified phosphorylation sites at Ser242/Ser244 (Figure 3B) and also found that these residues exhibited an LPS-inducible increase in phosphorylation, more so in NL than in TL cells (Figures S4A and S4B). Furthermore, phosphorylation of these sites was increased approximately 30% in the OA-treated TL cells (Figure 3C) compared to NL cells in which OA had little effect, suggesting that constitutively active PP2Ac targets these

Figure 1. PP2Ac Enhances Its Association with MyD88 and Shows a MyD88-Dependent Activation in ET Macrophages
(A) Experimental design of the AACT-based quantitative proteomics for phenotypic compositional screening of the MyD88 interactomes under N, NL, and TL.
(B–H) Mass spectra of the AACT-containing peptides of MyD88 and indicated TL-specific MyD88 interactors (B). Shown for each protein is one spectrum representative of at least two peptides sequenced by MS/MS. The PP2Ac activity was measured by phosphatase assay in RAWs (C), in WT and $MyD88^{-/-}$ BMDMs under N, or NL, or T, or TL (D), stimulated by CpG (E), by Poly (I:C) (F), by non-TLR stimuli including LPS-conditioned medium, TNF-α, and IR (G), agonist/cytokine-induced, time-dependent changes of PP2Ac activity and p-p65 (H). Each bar represents the mean ± SD of triplicates (same in figures below).
See also Figure S1.
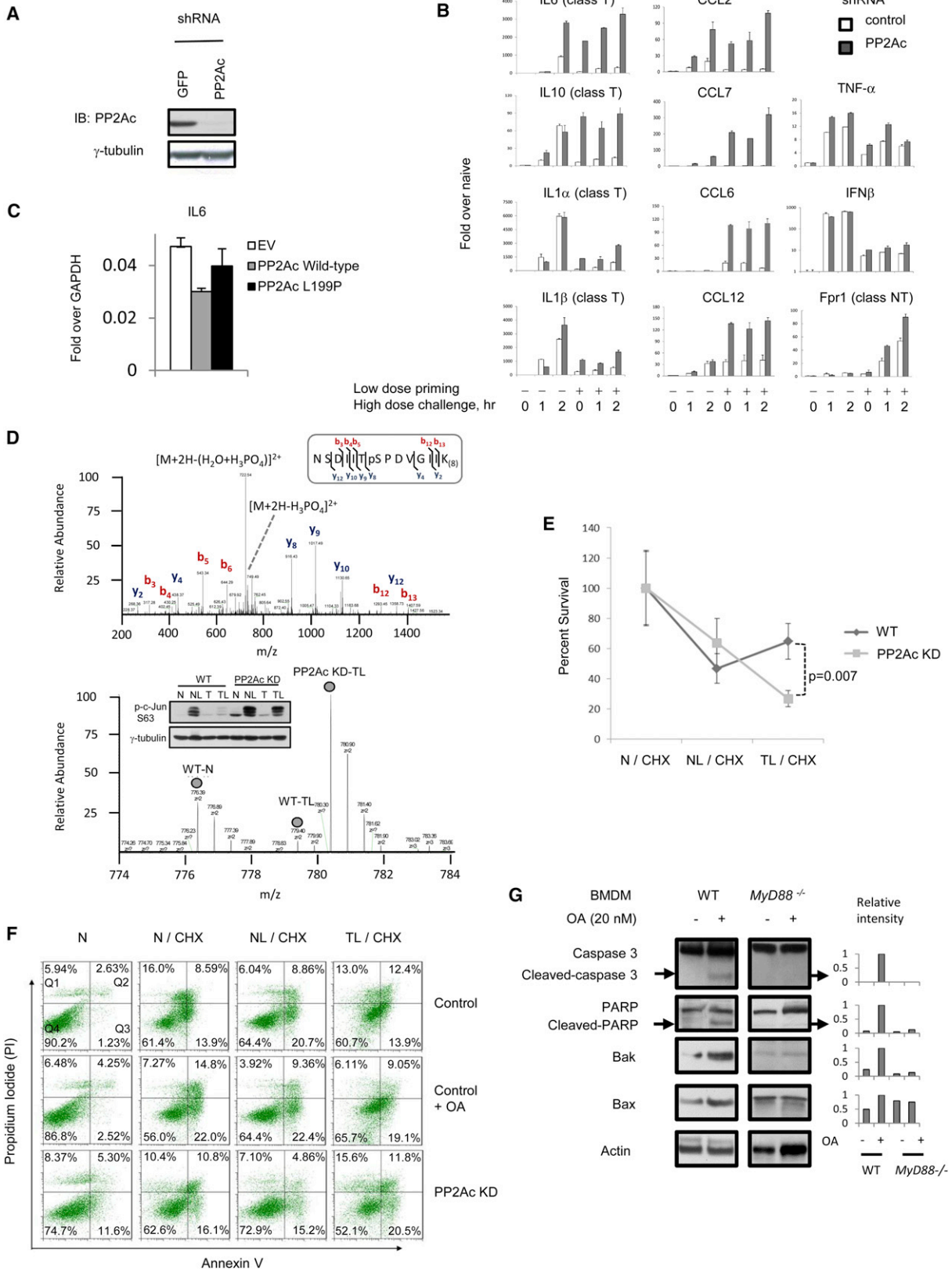
(legend on next page)

phosphoserines for dephosphorylation. Thus, we generated single (S242A and S244A) and double (S242A-S244A) nonphosphorylatable mutants of MyD88 and found that constitutively active PP2Ac associated more strongly with WT MyD88 than with any nonphosphorylatable mutant (Figure 3D), accordingly validating these PP2Ac-recognizing sites in TL cells. Because these serines reside in the TLR4-interacting MyD88 Toll/IL-1 receptor (TIR) domain that is critical for initiating proinflammatory signaling (Wang et al., 2006), we reasoned that these LPS-inducible, PP2Ac-target phosphorylations are essential for stability of the signal-promoting MyD88-TLR4 complex. Thus, we examined the LPS-induced, time-dependent TLR4-MyD88 association, which reached its highest strength at 15 min following LPS stimulation before returning to the basal level 24 hr after stimulation (Figure 3E, left). We then generated an phospho-Ser242 antibody (Figure S4C) to assay the time-dependent level of this proinflammatory MyD88 phosphorylation (pSer242) that also reached the highest level at 15 min and was reduced with prolonged LPS stimulation (Figure 3E, middle). We then compared binding of TLR4 to WT MyD88 versus each mutant in cotransfected cells stimulated by LPS for 15 min. Compared with WT MyD88, binding of each nonphosphorylatable mutant to TLR4 was not only weaker but also not LPS inducible (Figure 3E, right). These results together revealed that site-specific phosphorylation(s) in the MyD88 TIR is directly involved in the proinflammatory TLR4-MyD88 interaction, also demonstrating the physiological accuracy of our quantitative proteomic method for identification of these sites with 20 nM OA treatment.

To determine the impact of the PP2Ac-mediated MyD88 dephosphorylation on T class gene regulation, we transfected WT and the nonphosphorylatable MyD88 mutants into $MyD88^{-/-}$ BMDMs. Coincident with the weakened binding of MyD88 mutants to TLR4 (Figure 3E), following a high-dose Pam3CSK4 stimulation (MyD88-dependent TLR2 agonist), a 50% reduction in TNF-α was observed for the mutant-expressing cells compared to cells expressing WT MyD88 (Figure 3F). Clearly, disruption of the phosphorylation-dependent TLR4-MyD88 complex by constitutively active PP2Ac directly contributes to suppression of T class genes.

Constitutively Active PP2Ac Colocalizes with MyD88 in the Nuclei of Tolerant Macrophages

Given that constitutively active PP2Ac facilitates the departure of MyD88 from the TLR4 complex through site-specific dephos-

phorylation that often regulates protein translocation (Deribe et al., 2010), we then determined the ET-specific distribution of MyD88 and PP2Ac. Compared to their subcellular distributions in proapoptotic NL cells, both MyD88 and PP2Ac showed coincidently increased presence in the nuclei of the TL, prosurvival WT BMDMs (Figure 3G), in line with a previous report that MyD88 was preferentially in nuclei of nonapoptotic cells (Jaunin et al., 1998). Furthermore, immunoblotting revealed that more MyD88 and PP2Ac were retained in the nuclei of LPS-tolerant WT BMDMs than in naive cells (Figure 3H). In contrast, in the PP2Ac KD cells under TL, MyD88 failed to accumulate in nuclei. Similarly, OA-mediated PP2Ac inhibition reversed survival-characteristic retention of MyD88. Immunofluorescence staining further indicated that more PP2Ac and MyD88 colocalized in nuclei of TL WT macrophages than those in nonstimulated cells (Figure 3I, yellow spots in the nuclei area), all indicating that chronic-active PP2Ac promotes survival-specific translocation of MyD88 to ET nuclei through MyD88 dephosphorylation.

Constitutively Active PP2Ac Plays a MyD88-Dependent Role in Establishing the Gene-Specific Chromatin Modifications Responsible for Acquiring ET

We next explored the impact of the nuclear MyD88/PP2Ac accumulation on T class gene regulation. First, along with increasing PP2Ac in ET nuclei, the LPS-inducible increase of phospho-p65 was significantly suppressed in TL WT cells (Figure 3G, left lanes 2–4). Either PP2Ac KD or OA treatment dramatically reversed the TL-specific suppression of p-p65, indicating that constitutively active PP2Ac specifically dephosphorylates p-p65. Additionally, although p-p65 was suppressed, p65 was even higher in TL nuclei, indicating abnormal nuclear retention of nonphosphorylated p65 under ET. We then clarified the impact of PP2Ac-mediated p65 dephosphorylation on NFκB-regulated T class genes and its MyD88 dependence: in contrast to the MyD88-dependent suppression of IL6/IL10 in the TL WT BMDMs, OA inhibition of PP2Ac activity reactivated their release under LPS stimulation, even more so with Pam3CSK4 treatment for MyD88-dependent pathways (Figure 4A), all suggesting that, in a MyD88-dependent manner, constitutively active PP2Ac renders NFκB-dependent genes unresponsive by dephosphorylating nuclear p65 in ET macrophages.

Additionally, our phosphoproteomic findings of PP2Ac-target chromatin assembly/remodeling factors such as SWI/SNF (Figure S3B) implied that nuclear translocated, constitutively active PP2Ac directly participates in gene-specific chromatin

---

Figure 2. Constitutively Active PP2Ac Promotes Immunosuppression and Cell Survival

(A) PP2Ac abundance in the WCL of WT PP2Ac (GFP) or PP2Ac KD RAWs. IB, immunoblot.

(B) Releases of selected cytokines/chemokines were measured by qPCR for WT or PP2Ac KD cells under different inflammation conditions. The stimulated cells were collected at 1–2 hr after high-dose stimulation.

(C) RT-PCR was used to monitor the IL6 releases from the PP2Ac KD RAWs transfected with WT or L199P DN PP2Ac under TL (normalized by GAPDH mRNA).

(D) MS/MS sequencing spectrum of the p-Ser63 c-Jun peptide and MS of its quantitative changes in paired WT versus PP2Ac KD RAWs under N, NL, and TL, validated by immunoblotting (inset view).

(E) Comparative colony counts on paired WT versus PP2Ac KD RAWs under N, NL, and TL. Cells were costimulated by 1 μg/ml LPS with 1 μg/ml CHX for 12 hr (NL/CHX), or tolerized before CHX treatment and a high-dose LPS challenge (TL/CHX). p Value as indicated.

(F) Flow analysis of cell viability of the same set of (E) RAWs. The apoptotic cells were gated in Q3/Q2.

(G) Immunoblot analysis of caspase-9, caspase-3, PARP (a substrate of caspase-3), and expression of proapoptotic Bak and Bax in the TL WT (left panel) or $MyD88^{-/-}$ (right panel) BMDMs. Immunoblot intensities were quantified by a densitometry.

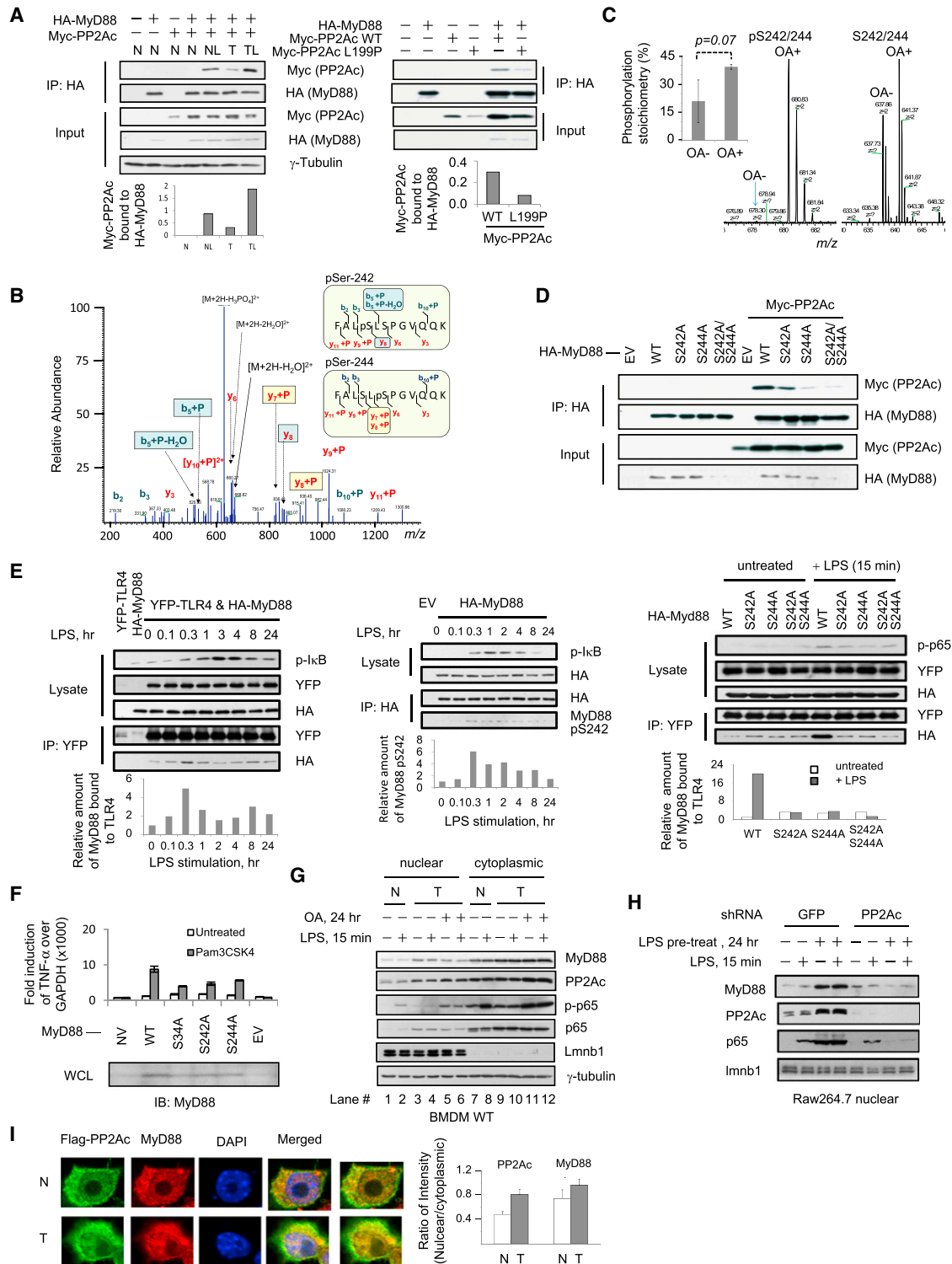See also Figures S2, S3, and Table S1.

Figure 3. Chronic-Active PP2Ac Dephosphorylates MyD88 for Dissociating Proinflammatory TLR4-MyD88 Complex and Promoting Its Cotranslocation with MyD88

(A) Immunoblot analysis of the immunoprecipitates from the TLR4 stable 293 cells cotransfected with MYC-tagged PP2Ac and HA-tagged MyD88 fused with GyrB (MyD88-GyrB) under N, NL, or TL (Left). HA-MyD88-GyrB was cotransfected with either MYC WT or DN PP2Ac construct, respectively, into the TLR4 stable cells that were induced to TL (Right).

(B) MS/MS spectrum of the phosphorylated S242 or S244 MyD88 peptide.

(legend continued on next page)

modifications. First, because histone H3 Ser10 phosphorylation (H3pS10) reflects the accessibility of NFκB to T class genes and mediates NFκB-dependent transactivation of these genes (Saccani et al., 2002), we determined whether constitutively active PP2Ac affects this proinflammatory epigenetic marker. Compared with its NL-enhanced but TL-suppressed nature in irritated WT cells, H3pS10 remained high in PP2Ac KD cells under NL or TL (Figure 4B), indicating that constitutively active PP2Ac specifically targets H3pS10. Furthermore, the LPS-inducible H3pS10 under NL was fully suppressed in TL WT BMDMs and was reversed by OA pretreatment, whereas no such OA effect was observed for NL cells (Figure 4C). As well, no detectable change due to OA treatment was observed in MyD88$^{-/-}$ BMDMs under TL, all indicating that in a MyD88-dependent manner, constitutively active PP2Ac dephosphorylates H3pS10 to selectively restrict accessibility of NFκB to T class gene promoters.

We then determined the link of the PP2Ac-coordinated MyD88 signaling to two major characteristics of the gene-specific regulation, histone deacetylation and inhibition of chromatin remodeling, at T class gene promoters under TL (Foster et al., 2007). First, the reversed suppression of IL6 and IL10 in the TL WT BMDMs pretreated with a HDAC inhibitor (SAHA) was not observed in the TL MyD88$^{-/-}$ cells (Figure 4D), indicating that histone deacetylation is MyD88 dependent. Second, levels of both p-Ser10 and acetyl-lysine 9 on H3 showed similar OA-triggered MyD88-dependent changes (Figure 4C), indicating that in the MyD88 interactome, constitutively active PP2Ac negatively regulates histone acetylation in a phosphorylation-dependent manner.

In combination, our findings of MyD88-dependent, PP2Ac-mediated p65 dephosphorylation and PP2Ac-target HDAC1 and chromatin remodeling complexes (Figure S3B) suggested that, in a phosphorylation-dependent manner, constitutively active PP2Ac directly regulates TLR4-induced recruitment of chromatin remodeling complexes to T class gene promoters, a process that is inhibited in tolerant macrophages. Thus, we examined the effect of PP2Ac KD on recruitment of an ATP-dependent chromatin remodeling complex, Brg1, to T class promoters, which was found suppressed under TL (Foster et al., 2007). As revealed by ChIP experiments, either PP2Ac KD or OA-mediated PP2Ac inhibition similarly reversed the ET-specific suppression of Brg1 recruitment to the IL6 and Lipg promoters

(Figure 4E). Furthermore, this proinflammatory recruitment was heavily suppressed in the TL WT BMDMs but suppressed to a much lower degree in the TL MyD88$^{-/-}$ BMDMs (Figure 4F). By contrast, whereas OA had little effect on Brg1 in the NL WT BMDMs, the TL WT BMDMs pretreated with OA showed greater Brg1 recruitment. However, this OA-initiated Brg1 recruitment was not observed in the TL MyD88$^{-/-}$ BMDMs. These results indicated that constitutively active PP2Ac cotranslocated with MyD88 negatively regulates the chromatin modification/remodeling required for T class gene transactivation.

DISCUSSION

Here, we have revealed a mechanism by which TLR4-induced, constitutively active PP2Ac broadly intersects with multiple, MyD88-dependent, interconnected signaling pathways and epigenetic regulation programs at both signal-specific and gene-specific levels for controlling inflammation as macrophages acquire ET. At the signaling level, because PP2Ac-targeted p-Ser242/p-Ser244 localize to the highly accessible area close to the conserved lymphoma-associated, survival-promoting Leu-265 (Ngo et al., 2011), we rationalized that under TL conditions with a lymphoma-mimicking chronic inflammatory environment, PP2Ac-mediated dephosphorylation of these residues could generate charge changes in the MyD88 TIR domain (Ohnishi et al., 2009) (Figure 4G), similarly leading to a weakened MyD88-TLR4 association and impaired proinflammatory and proapoptotic programs with reduced sensitivity to apoptotic stimuli. Consequently, the dissociating MyD88 from the TLR4 complex was translocated along with constitutively active PP2Ac into the nuclei of tolerant macrophages, indicative of increased cell survival (Figure 4H). At the chromatin level, constitutively active PP2Ac initiated the removal of phosphorylation-dependent acetylation, established T gene-specific chromatin modification, and suppressed the phosphorylation-dependent, Brg-mediated nucleosome remodeling for silencing of T class genes (Figure 4H).

From the perspective of a dynamic system, we have established a direct link between gene-specific and signal-specific regulation coordinately for the control of chronic inflammation, elucidating how the differential regulation of proinflammatory versus antimicrobial genes at the chromatin level is achieved. Of clinical relevance, the specific protein interactions in the

(C) Effects of PP2Ac inhibition on the LPS-inducible S242/S244 phosphorylation of the MyD88 IP from the TLR4 stable cells under NL or TL. (Right) MS spectra of this peptide with or without p-S242/p-S244. (Left) The fold change of phosphorylation caused by OA (y axis) under TL calculated in Figure S3B.
(D) MYC-PP2Ac was cotransfected with the construct of HA-WT or a nonphosphorylatable mutant MyD88 into the TLR4 stable cells before TL induction for immunoblot analysis.
(E) (Left) LPS-induced, time-dependent bindings between YFP-tagged TLR4 and WT MyD88. (Middle) The level of pSer242 in LPS-induced, time-dependent TLR4-MyD88 complexes blotted by pSer242 antibody. (Right) Comparative bindings of TLR4 to either WT or nonphosphorylatable mutants of MyD88 in the TLR4 stable cells following 15 min LPS stimulation.
(F) (Top) MyD88$^{-/-}$ BMDMs were infected by retrovirus that packaged each of the constructs containing WT, S242A, S244A, and S34A MyD88 and then stimulated by Pam3CSK4 for 1 hr. TNF-α mRNA was measured by RT-PCR for each MyD88-expressing BMDM without or with stimulation. EV, empty retrovirus; NV, noninfected MyD88$^{-/-}$ control. (Bottom) MyD88 expression in non- or transfected MyD88$^{-/-}$ BMDMs.
(G) Cytoplasmic and nuclear distributions of MyD88, PP2Ac, and p65 in BMDMs under N, NL, T, and TL; Lmnb1 as a nuclear marker.
(H) Immunoblot analysis of the nuclear fraction of PP2Ac KD or WT RAWs.
(I) Confocal microscopy of the subcellular colocalization of MyD88 and PP2Ac. The bar blot shows the ratio of the intensity of green or red fluorescence in nuclei versus that in cytoplasm, ten spots with the same square of area for each compartment.
See also Figure S4.
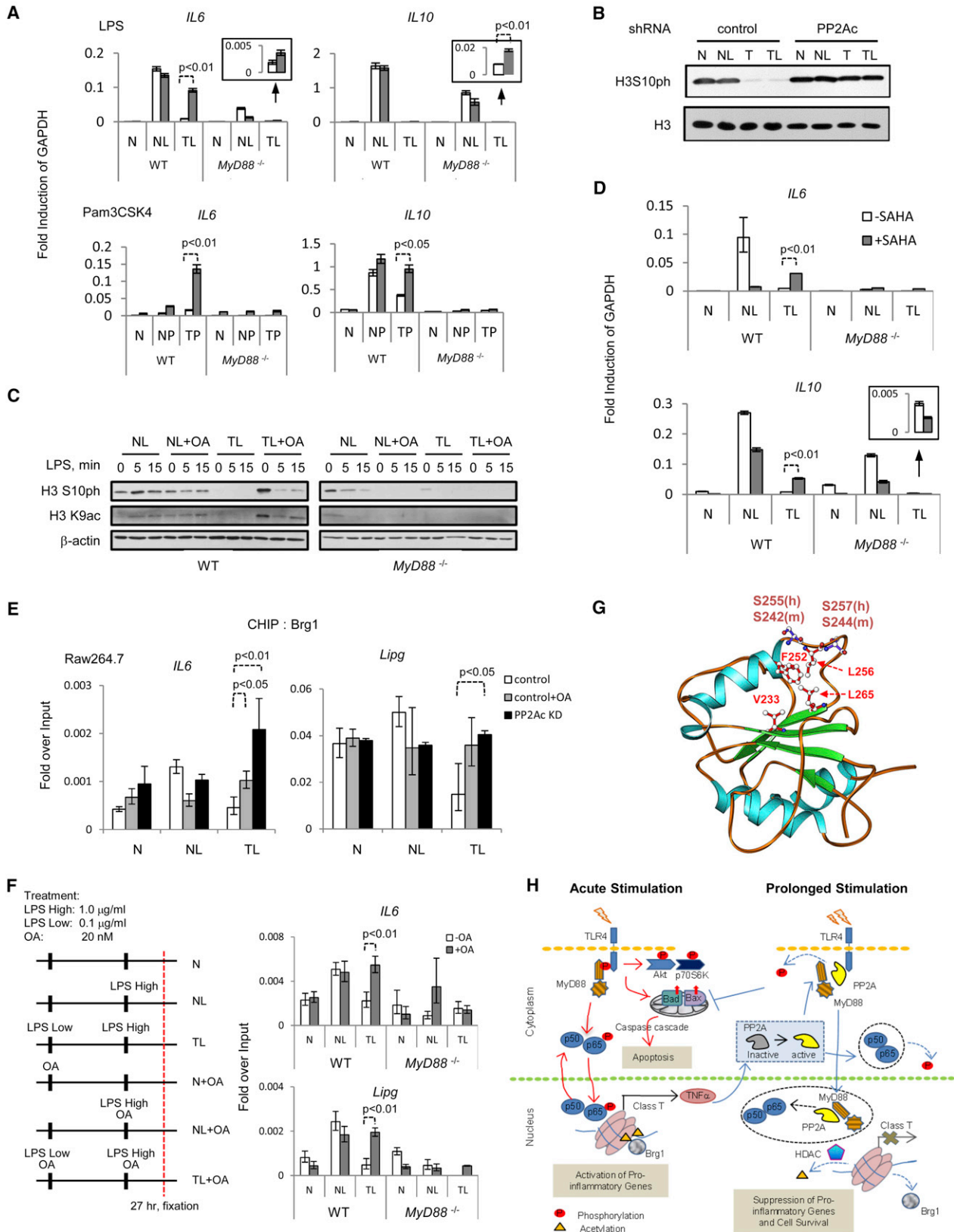
(legend on next page)

tolerance-specific MyD88 interactome coordinated by constitutively active PP2Ac that we have dissected may be targeted to unleash or attenuate cellular inflammatory responses. This knowledge is critical to better understand how MyD88 signaling produces diverse pathologic outcomes, including tissue repair and carcinogenesis, under different inflammatory conditions.

EXPERIMENTAL PROCEDURES

Proteomic Identification of TL-Specific MyD88 Interactors

The details about sample preparation, nano-LC-MS/MS analysis, and AACT-based quantitative proteomic identifications of NL- or TL-specific MyD88-interacting partners are given in Extended Experimental Procedures.

BMDM Stimulation and OA or SAHA Treatment

LPS stimulations of differentiated BMDMs were similar as to RAWs. In Pam3CSK4 stimulations, the priming dose was at 50 ng/ml, and a high dose was 500 ng/ml. SAHA was introduced into media 24 hr before stimulation, and 20 nM OA was added along with the stimuli.

PP2A Activity Assay

PP2Ac was IP using PP2Ac antibody with protein A agarose from 0.5–1.0 mg of each lysate of differentially stimulated cells. The phosphatase activity of IP PP2Ac was measured by the Phosphatase Assay Kit (Millipore) and normalized based on the amount of PP2Ac in the IP products.

Generation of the RAW Stable Lines with Either shRNA-GFP or -PP2Ac

The lentiviral plasmids pLKO.1 expressing the shRNA-PP2Ac targeting sequences 5′-CCAGATACAAATTACCTGTT-3′ and 5′-CGACGAGTGTTTAAG GAAATA-3′ were purchased from Thermo Scientific. To produce virus, pLKO.1-shRNA plasmids were cotransfected into 293T cells with ViraPower Mix (Invitrogen) by jetPRIME in vitro DNA and siRNA transfection reagent (Polyplus). Pseudovirus in supernatants was collected after 48 hr following transfection and used to transduce RAWs by spinoculation. Forty-eight hours after transfection, 8 μg/ml puromycin was added to select puromycin-resistant clones. Stable clones were maintained in the media containing 4 μg/ml puromycin.

Identification of LPS-Inducible, PP2Ac-Target Phosphorylations at MyD88

Due to the low abundance of endogenous MyD88 in RAW cells, few phosphorylation sites could be identified/quantified for their LPS-inducible changes. Therefore, quantitative proteomic identification of phosphorylation sites on MyD88 and the analysis of LPS or OA effects on these sites were conducted on the AACT-tagged HEK293 cells stably expressing TLR4-MD2-CD14. The details are given in Extended Experimental Procedures.

Retrovirus Infection and Cytokine Assay

Each cDNA of WT MyD88 or a MyD88 mutant was inserted into the MIG vector (Wang et al., 2010). Viral particles were generated in 293T cells and infected bone marrow cells three times. Five days after infection, matured BMDM cells were processed for LPS stimulation as described above.

Analysis of LPS-Induced Binding between TLR4 and WT or Mutant Myd88

HEK-TLR4 stable cells were cotransfected with both YFP-TLR4 and HA-WT or a mutant MyD88 by using jetPRIME. The cells were stimulated with 1 μg/ml LPS for indicated time and harvested. The cells were lysed in the buffer (50 mM Tris [pH 8.0], 150 mM NaCl, 1 mM EDTA, 1% Triton 100-X, protease inhibitor, and phosphatase inhibitors; Sigma-Aldrich). One milligram lysate was incubated with the anti-GFP IgG coupled on protein A magnetic beads for coIP and immunoblotting.

All procedures involving wild-type (WT) and *MyD88*⁻/⁻ knock-out mice have been approved by the University of North Carolina Animal Care and Use Committee.

SUPPLEMENTAL INFORMATION

Supplemental Information includes four figures, two tables, and Extended Experimental Procedures and can be found with this article online at http://dx.doi.org/10.1016/j.celrep.2013.01.029.

LICENSING INFORMATION

ACKNOWLEDGMENTS

Figure 4. Chronic-Active PP2Ac Directly Participates in TLR-Induced, MyD88-Dependent, Gene-Specific Chromatin Modifications

(A) A high or priming dose of LPS (L) or Pam3CSK4 (P) was respectively used to induce acute or chronic inflammation. Cells were harvested at 1 hr after stimulation, and *IL6* and *IL10* were quantified by quantitative RT-PCR and normalized with GAPDH. p values are as indicated.

(B) Immunoblot analysis of pSer10 H3 in WT or PP2Ac KD RAWs under N, NL, T, and TL.

(C) LPS-induced changes of pSer10 H3 or acetylated H3 in WT or MyD88⁻/⁻ BMDMs.

(D) Cells were treated by 2 μM SAHA for 24 hr prior to stimulation. Similar to (A), *IL6/IL10* mRNAs were measured for those isolated from the WT or *MyD88*⁻/⁻ BMDMs with indicated treatment(s).

(E) WT or PP2Ac KD RAWs with indicated treatment(s) were fixed with DSG/formaldehyde 3 hr after stimulation and analyzed by ChIP (Brg1). qPCR was normalized to INPUT.

(F) WT or *MyD88*⁻/⁻ BMDMs with indicated treatment(s) were analyzed by ChIP (Brg1).

(G) Location of serine phosphorylations in the MyD88 TIR domain. S242(m) and S244(m) are the mouse counterparts (NP_034981) of human S255(h) and S257(h) (NP_002459).

(H) The mechanistic model for the MyD88-dependent, PP2Ac-coordinated control of the inflammation.

See also Figures S3 and S4.

REFERENCES

Chang, H.Y., Jennings, P.C., Stewart, J., Verrills, N.M., and Jones, K.T. (2011). Essential role of protein phosphatase 2A in metaphase II arrest and activation of mouse eggs shown by okadaic acid, dominant negative protein phosphatase 2A, and FTY720. J. Biol. Chem. *286*, 14705–14712.

Chen, X., Smith, L.M., and Bradbury, E.M. (2000). Site-specific mass tagging with stable isotopes in proteins for accurate and efficient protein identification. Anal. Chem. *72*, 1134–1143.

Dai, P., Jeong, S.Y., Yu, Y., Leng, T., Wu, W., Xie, L., and Chen, X. (2009). Modulation of TLR signaling by multiple MyD88-interacting partners including leucine-rich repeat Fli-I-interacting proteins. J. Immunol. *182*, 3450–3460.

Deribe, Y.L., Pawson, T., and Dikic, I. (2010). Post-translational modifications in signal integration. Nat. Struct. Mol. Biol. *17*, 666–672.

Drexler, S.K., and Foxwell, B.M. (2010). The role of toll-like receptors in chronic inflammation. Int. J. Biochem. Cell Biol. *42*, 506–518.

Foster, S.L., Hargreaves, D.C., and Medzhitov, R. (2007). Gene-specific control of inflammation by TLR-induced chromatin modifications. Nature *447*, 972–978.

Huang, B., Zhao, J., Unkeless, J.C., Feng, Z.H., and Xiong, H. (2008). TLR signaling by tumor and immune cells: a double-edged sword. Oncogene *27*, 218–224.

Jaunin, F., Burns, K., Tschopp, J., Martin, T.E., and Fakan, S. (1998). Ultrastructural distribution of the death-domain-containing MyD88 protein in HeLa cells. Exp. Cell Res. *243*, 67–75.

Junttila, M.R., Li, S.P., and Westermarck, J. (2008). Phosphatase-mediated crosstalk between MAPK signaling pathways in the regulation of cell survival. FASEB J. *22*, 954–965.

Kong, M., Fox, C.J., Mu, J., Solt, L., Xu, A., Cinalli, R.M., Birnbaum, M.J., Lindsten, T., and Thompson, C.B. (2004). The PP2A-associated protein alpha4 is an essential inhibitor of apoptosis. Science *306*, 695–698.

Lee, S.H., Hu, L.L., Gonzalez-Navajas, J., Seo, G.S., Shen, C., Brick, J., Herdman, S., Varki, N., Corr, M., Lee, J., and Raz, E. (2010). ERK activation drives intestinal tumorigenesis in Apc(min/+) mice. Nat. Med. *16*, 665–670.

Li, L., Feng, Z., and Porter, A.G. (2004). JNK-dependent phosphorylation of c-Jun on serine 63 mediates nitric oxide-induced apoptosis of neuroblastoma cells. J. Biol. Chem. *279*, 4058–4065.

Liew, F.Y., Xu, D., Brint, E.K., and O'Neill, L.A. (2005). Negative regulation of toll-like receptor-mediated immune responses. Nat. Rev. Immunol. *5*, 446–458.

Ngo, V.N., Young, R.M., Schmitz, R., Jhavar, S., Xiao, W., Lim, K.H., Kohlhammer, H., Xu, W., Yang, Y., Zhao, H., et al. (2011). Oncogenically active MYD88 mutations in human lymphoma. Nature *470*, 115–119.

Ohnishi, H., Tochio, H., Kato, Z., Orii, K.E., Li, A., Kimura, T., Hiroaki, H., Kondo, N., and Shirakawa, M. (2009). Structural basis for the multiple interactions of the MyD88 TIR domain in TLR4 signaling. Proc. Natl. Acad. Sci. USA *106*, 10260–10265.

Rakoff-Nahoum, S., and Medzhitov, R. (2007). Regulation of spontaneous intestinal tumorigenesis through the adaptor protein MyD88. Science *317*, 124–127.

Rakoff-Nahoum, S., and Medzhitov, R. (2009). Toll-like receptors and cancer. Nat. Rev. Cancer *9*, 57–63.

Saccani, S., Pantano, S., and Natoli, G. (2002). p38-Dependent marking of inflammatory genes for increased NF-kappa B recruitment. Nat. Immunol. *3*, 69–75.

Suzuki, T., Kobayashi, M., Isatsu, K., Nishihara, T., Aiuchi, T., Nakaya, K., and Hasegawa, K. (2004). Mechanisms involved in apoptosis of human macrophages induced by lipopolysaccharide from Actinobacillus actinomycetemcomitans in the presence of cycloheximide. Infect. Immun. *72*, 1856–1865.

Wang, T., Chuang, T.H., Ronni, T., Gu, S., Du, Y.C., Cai, H., Sun, H.Q., Yin, H.L., and Chen, X. (2006). Flightless I homolog negatively modulates the TLR pathway. J. Immunol. *176*, 1355–1362.

Wang, Y.Q., Souabni, A., Flavell, R.A., and Wan, Y.Y. (2010). An intrinsic mechanism predisposes Foxp3-expressing regulatory T cells to Th2 conversion in vivo. J. Immunol. *185*, 5983–5992.